JOURNAL OF MATERIALS SCIENCE 27 (1992) 1989–2000

Review
Advances in brazing of ceramics

O. M. AKSELSEN
The Welding Centre, SINTEF (Foundation for Scientific and Industrial Research at the Norwegian Institute of Technology), N-7034 Trondheim, Norway

The main parameters in direct brazing of ceramics to ceramics and to metals are reviewed, with primary emphasis on those influencing wetting of solid ceramics by liquid filler metals. In general, wetting of ceramics by conventional brazing alloys has been regarded as difficult. As a consequence, premetallization of the faying surfaces is frequently used to facilitate the brazing of ceramics. However, it is evident from the literature that recent developments in filler metals, based on active metal (e.g. Ti) additions (the amount depending on alloy composition and type of ceramic), have provided a basis for a substantial reduction of the contact angle. This favourable effect is caused by their reactivity, resulting in the formation of oxides when joining oxide ceramics (e.g. Al_2O_3), and nitrides or carbides and silicides in the case of non-oxide ceramics (e.g. Si_3N_4 or SiC). In addition to insufficient wetting, the mismatch in thermal expansion between the joint members may give rise to a low strength level due to the formation of high residual stresses on cooling. These stresses may limit the maximum allowable flaw size in ceramics to a few micrometres, i.e. of a similar size to that of pores.

1. Introduction

The application of ceramics in structural components such as turbine engines has received extensive attention in recent decades due to their excellent high-temperature strength and resistance to corrosion and wear. However, because of their brittle nature, joining of ceramics to metals is frequently required. As a consequence, the lack of joining techniques has in many cases limited their use. Normally, conventional fusion welding is not performed due to the risk of brittle fracture initiation as a result of the high contraction stresses formed on cooling. In addition, the high melting temperature of ceramics presupposes the use of high-power sources, which means that only laser and electron-beam welding are considered to be applicable. Moreover, silicon-based ceramics such as silicon carbide and nitride sublime without melting, and should therefore not be subjected to fusion welding at normal pressures. Alternatively, ceramic–metal joints may be obtained on the basis of adhesive bonding, although the strength may be reduced during long service. Hence, solid-state bonding and various types of brazing are currently applied to maintain the excellent base-material properties of ceramics.

In the case of brazing, ceramic–ceramic and ceramic–metal joints may be obtained in two different ways: (i) indirect brazing, where the ceramic surfaces are metallized prior to brazing with conventional filler metals; and (ii) direct brazing, where the filler alloys contain active elements such as titanium.

Brazing possesses a major advantage compared with conventional welding, as the base materials do not melt. This allows brazing to be applied in the joining of dissimilar materials which cannot be joined by fusion processes due to metallurgical incompatibility. In general, brazing produces less thermally induced stress and distortion since the entire component is subjected to heat treatment, thus preventing the localized heating which may cause distortion in welding. In addition, it is possible to maintain closer assembly tolerances without costly secondary operations. Moreover, brazing can be easily adopted for mass production.

In the present paper, the state of the art on direct brazing of ceramics to ceramics and to metals is reviewed, with primary emphasis on recent advances in the development of brazing filler metals to provide the required wetting and spreading on ceramic surfaces. Finally, the effects of operational parameters (temperature, time), as well as the mismatch in thermal expansion between the joint members, on the mechanical properties of ceramic–ceramic and ceramic–metal direct brazed joints are discussed.

2. Wetting and spreading

Equations predicting the form and spreading of liquid drops on a solid surface have been established on the basis of classical physical and chemical principles. A comprehensive theory of the spreading of liquids has been developed by Harkins [1]. Considering the fact that materials possess a free surface energy, the following energy balance will exist between a liquid drop and a solid substrate (Fig. 1a):

$$\gamma_{SL} = \gamma_{SV} - \gamma_{LV}\cos\theta \qquad (1)$$

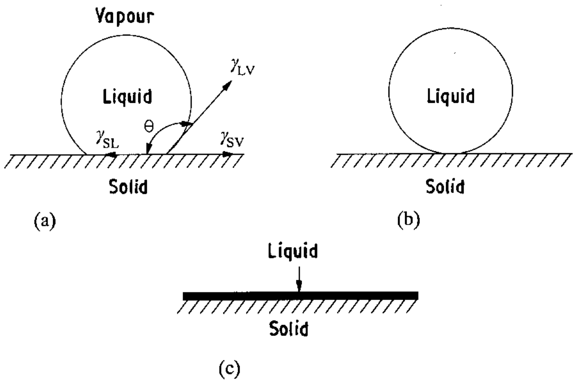

Figure 1 Principles of wetting: (a) definition of the wetting angle θ by surface-tension balance for a liquid drop on a solid surface (schematic), (b) no wetting and (c) complete wetting.

Here γ_{LV}, γ_{SL} and γ_{SV} denote the liquid–vapour, solid–liquid and solid–vapour surface tension, respectively, and θ represents the contact angle between liquid and solid (i.e. the wetting angle in brazing).

In order to obtain spreading, the following requirement should be met:

$$\gamma_{SL} < \gamma_{SV} - \gamma_{LV}\cos\theta \qquad (2)$$

It has been pointed out by Kingery [2] that a corresponding, necessary but not sufficient, condition for spreading is that the liquid–vapour interface energy must be lower than that of the solid–vapour interface ($\gamma_{LV} < \gamma_{SV}$).

From Equation 1 it follows that when γ_{SL} is larger that γ_{SV}, the value of θ is greater than 90° and no spreading occurs, i.e. the liquid drop tends to spheroidize (Fig. 1b). In contrast, when γ_{SL} is lower than γ_{SV} ($\theta < 90°$), the solid surface will be covered by a thin film of liquid, pulled along the surface by capillary forces (Fig. 1c).

In the case of ceramics, recent investigations indicate that wetting undergoes three main stages [3]:

Stage I: Initial or vibration stage
Stage II: Constant stage
Stage III: Decreasing stage

Stage I is characterized by dynamic and chemical non-equilibrium conditions due to vibrations of the liquid drop. Stage II represents dynamic but not chemical equilibrium, since the wetting angle is constant. The shift from stage II to stage III is determined by chemical and physical interactions at the ceramic–liquid metal interface. The extent of these interactions depends on diffusion and chemical reactions. This means that a state of chemical equilibrium is reached, resulting in a decrease in the wetting angle. Data obtained from the wetting of magnesia with liquid aluminium show that very long brazing times (approaching 10^4 s) are required to reach stage III. Yashimi *et al.* [3] suggested that the angle established during stage II should be reported in order to avoid overestimation of wetting. In practice, however, brazing is frequently limited to a maximum of say 1 h, indicating that reported wetting angles represent conditions for stage II and the transition between stages II and III. Moreover, the vibration stage is inherent in the sessile drop experimental technique, indicating that current procedures with preplacement of the brazing alloys allow chemical reactions to take place at an early stage. This means that the wetting angle starts to decrease after some delay, followed by an equilibrium stage where the angle is kept constant at a low level (< 10°).

In contrast to the wetting angle, the surface free energies are more difficult to measure. However, the value of γ_{SV} has been calculated from considerations of cleavage strength as the work done in separating two surfaces (see Lancaster [4]). Data available in the literature [5–15] suggest that the relationship between surface energy and temperature takes the general form

$$\gamma_{Me} = A - B(T - C) \qquad (3)$$

where A and B are constants, C is the melting temperature (in Kelvin) and T the absolute temperature.

Recent measurements, based on the study of pure metal sessile drops on oxide surfaces (Al_2O_3, MgO, CaO, SiO_2 and ZrO_2), resulted in the following relationships (γ in $mJ\,m^{-2}$) [15]:

$$\gamma_{Sn} = 551 - 0.09\,(T - 505) \qquad (4a)$$

$$\gamma_{Ag} = 910 - 0.17(T - 1234) \qquad (4b)$$

$$\gamma_{Au} = 1105 - 0.28(T - 1336) \qquad (4c)$$

$$\gamma_{Cu} = 1320 - 0.28(T - 1356) \qquad (4d)$$

Based on contact angle measurements and Equation 4, the work of adhesion may be calculated using the following formula (Young–Dupre equation):

$$W_{ad} = \gamma_{LV}(1 + \cos\theta) \qquad (5)$$

It should be noted that when joining materials with different thermal expansion, a subtraction term would be required to account for the negative contributions from strains. Moreover, the use of Equation 5 presupposes that the surface energy values of γ_{SV} and γ_{SL} are constant during the experiments.

It is seen from Equation 5 that the work of adhesion increases with increasing temperature due to a reduction of the contact angle. This implies that the bond strength is inversely proportional to the contact angle, which in fact has been verified experimentally (see later discussion).

From the literature, it is apparent that a considerable scatter in the free surface energy data has been found, particularly for gold and copper (a comparison of published data is contained in Nogi *et al.* [15]). It may be suggested that this scatter is associated with two main factors: (i) varying content of impurities, particularly surface-active elements which may alter the surface free energy considerably: and (ii) different oxygen potential in the atmosphere. In the latter case, it has been verified experimentally that the surface free energy is reduced with increasing partial pressure of oxygen, as shown for liquid drops of Cu on alumina in Fig. 2 (surface free energy between liquid and solid, γ_{SL}). Hence, when referring to Equation 2, a reduction in the value of γ_{SL} will enhance wetting and spreading, which means that the contact angle is reduced. This is confirmed by the data in Fig. 3, which

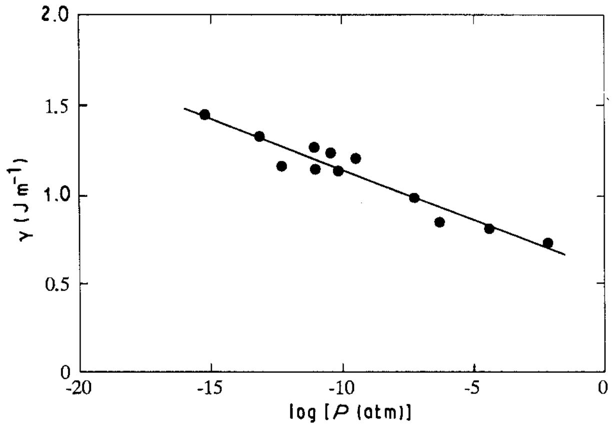

Figure 2 Effect of partial pressure p of oxygen on surface free energy γ between liquid Cu and solid Al_2O_3 (after O'Brien and Chaklader [16]).

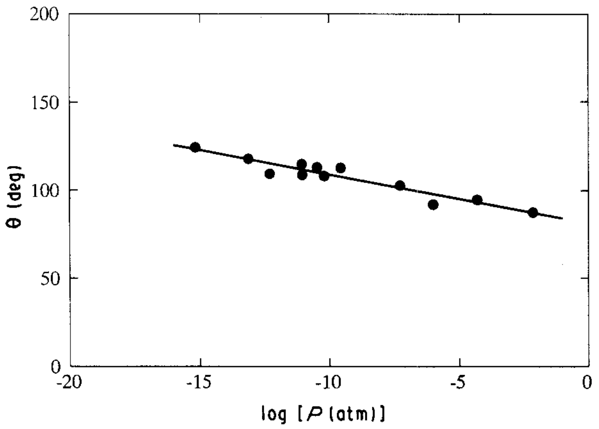

Figure 3 Effect of partial pressure p of oxygen on contact angle θ between liquid Cu and solid Al_2O_3 (after O'Brien and Chaklader [16]).

shows that the contact angle is reduced with increasing partial pressure of oxygen. Improved wetting was stated to be a result of the formation of $CuAlO_2$ on the liquid–solid interface. In most cases, however, the oxygen potential in the brazing atmosphere should be kept as low as possible to prevent active elements added to the filler metal from reacting with oxygen, which may give rise to a consequent loss in the wettability of ceramic surfaces.

So far, the analysis applies to flat surfaces only, which in practice do not exist. Surface energy measurements are all based on surfaces possessing a certain degree of roughness. The wetting and filling of brazed joints would be expected to be dependent on the roughness in two ways: (i) surface and interfacial energy changes are dependent on the real area over which the liquid flows; and (ii) roughness of the surfaces in the capillary gap may cause a transition from laminar to turbulent flow, resulting in an increased resistance to flow. Energy changes require knowledge of the ratio between the real and the apparent area, while the flow pattern is determined by the shape and probably by the height of the surface asperities. In the case of ceramics, their brittleness may facilitate the formation of small surface cracks, either from processing stages, or through manufacturing or surface preparation (e.g. grinding or polishing). The ratio between the real and the apparent area may be relatively high, resulting in large deviations from the theoretical analysis above. This fact has been verified for metals by Bowden and Rideal [17]. The effect of surface roughness may be taken into account by modifying Equation 1 [18]:

$$\gamma_{SL} = \gamma_{SV} - \gamma_{LV}\cos\delta \qquad (6)$$

where δ is the observed contact angle, related to θ by

$$\cos\delta = r\cos\theta \qquad (7)$$

Here, r is the ratio between the real and the apparent surface area.

In practice, Equation 1 will still be the one most frequently used since the real surface area is difficult to measure.

3. Development of active filler metals

3.1. Ag–Cu brazes

In the last two decades, the major impetus in brazing of ceramics has been the development of filler metals with improved wettability, eliminating the need for premetallization. These mainly consist of two groups of alloys, i.e. Cu–X [19–26] or Ag–Cu–X brazes [27–30], where X is typically a group IVB element (Ti, Zr, Hf), and Ti–Zr [31–33] alloys (often with additions of Be [31–34]). In many cases, active brazes also contain additions of Ni, Be, Cr, V, In and Co (e.g. [35–39]). In Ag-based alloys, the solubility of a metal such as Ti is relatively low at relevant brazing temperatures (950–1050 °C). In contrast, the solubility of Ti in Cu is much higher, which makes the combination of Ag and Cu attractive for many ceramics and ceramic–metal combinations. Hence, modern filler metals for brazing of ceramics contain active elements which promote wetting by decomposing a thin layer at the ceramic surface. The improved wetting of silicon nitride, silicon carbide and alumina as a result of titanium additions to the fillers is shown in Fig. 4. Apparently, about 10 at % Ti is sufficient to wet silicon nitride (1100 °C) and silicon carbide (1000 °C), while 30 at % is required to obtain a similarly low contact angle on alumina (1100 °C). It is reasonable to

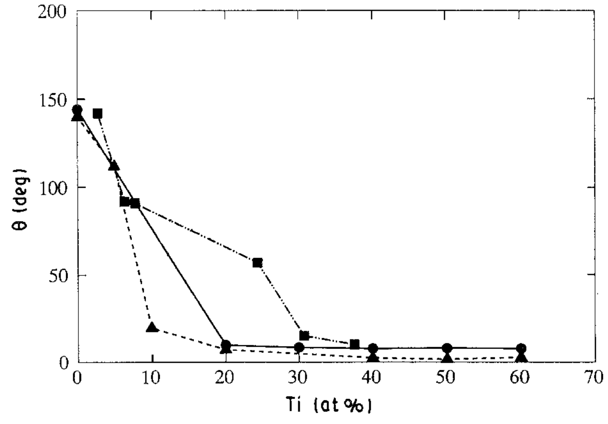

Figure 4 Effect of filler-metal titanium content on contact angle θ (data from [25], [40] and [41] for (●) Si_3N_4 (1100 °C), (▲) SiC (1000 °C) and (■) Al_2O_3 (1100 °C), respectively).

suggest that this observation is closely linked to the higher thermodynamical stability of aluminium oxide. As a consequence of the low solubility of Ti in Ag, the use of Ag–Cu-based alloys should be recommended when brazing alumina, while Ag-based alloys provide a sufficiently high amount of Ti in the case of silicon nitride and silicon carbide.

It should also be noted that wetting of ceramics has been found to be dependent on the processing technique, as shown for SiC by Iseki *et al.* [42]. Their data showed that reaction-sintered specimens required a higher Ti content than those which were pressureless-sintered. An attempt to explain these differences has not yet been made. However, the pressureless-sintered SiC contained small amounts of free carbon atoms, suggesting a higher rate of reaction between Ti and free C compared with that of Ti and SiC. Favourable effects of titanium have also been reported for zirconia [29, 43], and various metal–Al_2O_3 joints [36, 44, 45].

The Ag–Cu–Ti alloys are based on titanium additions to the eutectic composition of Ag–Cu (78 at % Ag–22 at % Cu), which provides sufficient fluidity of the alloy, since the melting range is relatively narrow. The addition of Ti to Ag–Cu alloys results in minor changes of the melting temperature only (T_M between 750 and 850 °C), which is essential to avoid high-temperature brazing due to the residual stress problem. The binary Cu–Ti alloys solidify over a narrow temperature range (<60 °C), with the exception of those alloys which contain less than 10 at % Ti. This improves the flowability and reduces the risk of liquation and brittleness during solidification. Moreover, the recent developments made in rapid solidification of metals may provide a basis for further improvements in the fabrication of brazing fillers. On this basis, alloys can be made available with chemical compositions outside the range in which is possible to fabricate with conventional casting technology.

3.2. Al brazes

In addition to titanium and zirconium, attempts have been made to develop aluminium-based alloys [46–51]. The results indicate that the contact angle on alumina is relatively high compared with that of titanium-containing alloys. Considering the low surface free energy of liquid pure aluminium at the melting temperature, a relatively low work of adhesion may occur. This observation implies that brazing with aluminium fillers may require a high temperature (minimum 1050 °C), as shown by Fig. 5. For practical purposes, a contact angle between 70 and 90° may be insufficient to provide satisfactory spreading, and hence a low bond strength level may appear. As a consequence, the use of such fillers may be critical. On the other hand, wetting of alumina can be enhanced by additions of copper to the aluminium filler. In this situation, the contact angle approaches 50° for copper amounts between 4 and 30 wt % [52]. Within this range of Cu content the solidification range is between 0 and 200 °C, and no intermetallic phases are formed (these are connected with the Cu-rich side of the Al–Cu binary system). A similar contact angle has been observed in the wetting of zirconia at 1100 °C (>1000 s), using Al–Cu alloys with 0–7 wt % Cu [53].

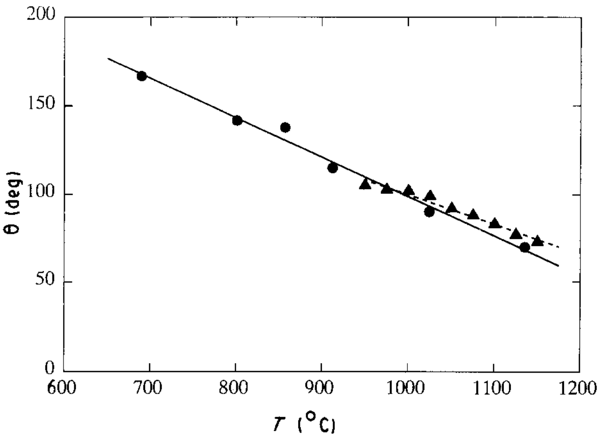

Figure 5 Effect of brazing temperature T on contact angle θ between liquid aluminium and solid alumina (after (●) Wolf *et al.* [48] and (▲) Champion *et al.* [50]).

3.3. Sn solders

Brazing fillers with additions of titanium and zirconium have been designed to meet the stringent service requirements (high temperature) of many metal–ceramic joints. In many cases, however, the service temperature is much lower than, say 600 °C (e.g. in electrical feed-throughs). According to Kapoor and Eagar [54, 55], the development of tin-based brazes with a lower melting temperature than Ag- and Cu-based fillers would minimize the residual stresses. Although their results from wetting angle measurements show that a brazing temperature of at least 900 °C is required (Fig. 6), the lower solidification temperature may reduce the residual stress problem, provided that the solidification range is sufficiently small. It may be tentatively suggested that titanium additions beyond 2 at % should be avoided due to the substantial increase in the solidification range between 4 and 40 at % Ti (from about 180 to about 650 °C [56]). This may reduce the flowability of the brazing

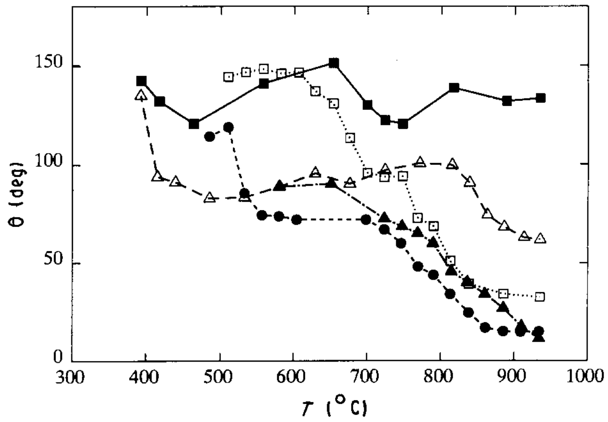

Figure 6 Effect of temperature T and alloy composition on contact angle θ between liquid metal and silicon nitride (after Kapoor and Eagar [54]): (■) 0.5% Ti, (●) 2% Ti, (▲) 5% Ti, (□) 7% Ti, (△) 5% Zr.

alloy, and hence reduce the spreading. As a consequence, insufficient joint strength may result. At present, this suggestion cannot be verified due to the lack of data from mechanical testing. An inspection of Fig. 6 also indicates, for a similar concentration, that titanium is more effective than zirconium, in spite of the fact that Zr has the highest affinity to nitrogen. This is also the case for copper-based Ti- or Zr-containing alloys [23]. From the literature [57], the data on Cu–X and Ag–X alloys reveal that X–Ti heats of solution are less negative than those of X–Zr alloys (X is Cu, Ag). Hence, the lower wettability observed for Zr was proposed to be caused by its lower activity, i.e. higher affinity for matrix elements (Cu, Ag, Sn) [54]. Presumably, this may be linked to a lower solid solubility of Zr in Sn, resulting in extensive compound formation on solidification, identified as Sn_2Zr intermetallic particles by Kapoor and Eagar [54]. The volume fraction of Sn_2Zr within the Sn alloy was reported to be greater than the corresponding one for Sn_5Ti_6 in Sn–Ti alloys. In addition, the intermetallic layer (rich in either Zr or Ti) was smaller for the Sn–Zr alloy. Considering the slower growth rate of the reaction layer for Zr-containing brazes, it may be suggested as an alternative hypothesis that the diffusivity of Zr is lower than that of Ti. Based on results obtained from brazing of Si_3N_4 to refractory metals (W, Mo, Ta and Nb) with Cu–5% Ti and Cu–10% Zr [58], a higher apparent activation energy for reaction layer growth was calculated for the latter alloy. Determination of diffusion data for Sn-based solders would therefore be a subject for further work.

The application of brazing alloys which contain reactive metals requires that joining is performed in a vacuum with a very low oxygen potential, or in a dry inert-gas atmosphere with a low dew point to prevent the active elements from reacting with the atmosphere. If these requirements cannot be met, the ceramic surfaces should be metallized prior to brazing. Several techniques are available, such as thermal spraying, electrolytic coating, electron-beam and laser coating, vapour-phase deposition (chemical or physical) and hot isostatic pressing. The techniques most commonly used are, however, the moly–manganese [59–66] and the metal hybride powder processes [67]. Joining of metallized ceramics can subsequently be performed with conventional brazing alloys (typically BĈu, BAg and BAu alloys according to the American Welding Society Specification AWS A5.8.89, 1989).

4. Interface chemical reactions

In the brazing of premetallized ceramics to themselves or to metals, the reduction of metal oxides is essential to provide the required wetting and spreading. This may be obtained by

(i) the use of a reducing atmosphere (hydrogen, carbon monoxide, carbon dioxide or ammonia);

(ii) vacuum, often in combination with an inert gas, usually argon or nitrogen; or

(iii) the use of fluxes, often in combination with gas.

The mechanisms occurring in the reduction of oxides in the presence of fluxes are not yet fully clarified (see Milner's discussion [68]), although the indications are that an electrochemical process is involved. Modern alloys for direct brazing of ceramics contain a reactive component, eliminating the need for flux.

The type of atmosphere may be selected on the basis of thermodynamical considerations with respect to dissolution of the actual metal oxide present at the faying surface. For a detailed discussion of this subject, reference is made to the paper of Milner [68].

In contrast to the brazing of premetallized ceramics, the use of flux is not required in direct brazing. On the other hand, either high-purity inert gas or a vacuum (minimum 10^{-3}–10^{-4} torr) is recommended. A reducing atmosphere such as hydrogen should be avoided due to the high affinity between hydrogen and active metals, e.g. titanium.

The reactive elements in the filler react with the ceramic to form reaction layers constituting several phases at the base material–filler metal interface. An example is shown in Fig. 7 for the brazing of alumina to copper using a 50 at % Cu–50 at % Ti filler alloy. The reaction layer consists of a copper-rich phase with some titanium, together with the oxides TiO_x and $(Al, Ti)_2O_3$. Several oxide compositions are possible [69], such as the formation of TiO (γ-TiO, β-TiO, α-TiO and β-$Ti_{1-x}O$), Ti_2O_3, Ti_3O_5 and TiO_2 [70]. The latter form is the most stable one. The possible chemical reactions together with their free energy of formation are summarized in Table I.

Similar reactions would be expected to occur in the brazing of other oxide ceramics or in brazing with zirconium-containing filler alloys, although the free energy of formation may be different. As experienced

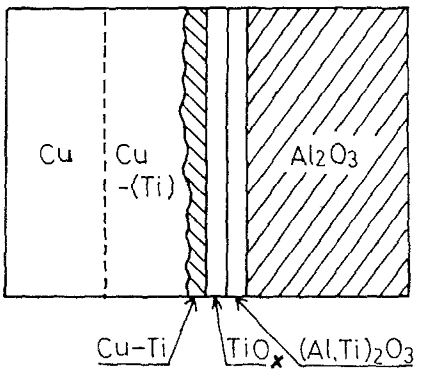

Figure 7 Reaction layer at the interface between Al_2O_3 and Cu (schematic) in direct brazing in vacuum with a 50 at % Cu–50 at % Ti filler alloy (after Naka *et al.* [69]).

TABLE I Possible reactions between titanium-containing fillers and oxide ceramics (standard Gibbs energies calculated from data given in [70, 71])

Reaction[a]	Free energy ($kJ\ mol^{-1}$)
$2\ Ti(s) + O_2(g) = 2\ TiO(s)$	$\Delta G^\circ = -1023 + 0.178T$
$\frac{4}{3}\ Ti(s) + O_2(g) = \frac{2}{3}\ Ti_2O_3(s)$	$\Delta G^\circ = -1001 + 0.172T$
$\frac{6}{5}\ Ti(s) + O_2(g) = \frac{2}{5}\ Ti_3O_5(s)$	$\Delta G^\circ = -975 + 0.171T$
$Ti(s) + O_2(g) = TiO_2(s)$	$\Delta G^\circ = -914 + 0.175T$

[a] The symbols g and s represent gas and solid states, respectively.

with TiO, the zirconium oxide ZrO_2 may have several compositions [71].

In the direct brazing of non-oxide ceramics such as silicon carbide and silicon nitride, the filler metal should contain elements with a high affinity to carbon and nitrogen to provide sufficient wetting. For titanium- or zirconium-containing alloys, the chemical reactions listed in Table II may occur between Si_3N_4 and filler metal [69]. The actual type of compound formed is dependent on both temperature and brazing alloy chemical composition. Such reactions are favourably affected by free silicon atoms in reaction-bonded ceramics, or by additives in pressureless-sintered ceramics. In addition, various copper silicides (γ-Cu_5Si, ε-$Cu_{15}Si_4$ and η'-CuSi are possible) may form since the reaction between Ti and nitrogen provides free silicon atoms.

Similar reactions, with carbides substituting nitrides, would be expected to occur in silicon carbide joints with Ti- or Zr-containing filler metals. In addition to silicides and TiC, Ti_3SiC_2 has been observed [74].

In the case of aluminium brazes, the reaction layer may consist of β'-sialon or AlN [75, 76] when joining Si_3N_4, while Al_4C_3 may form when joining SiC [74]. The formation of β'-sialon requires that oxygen is present in the brazing atmosphere, and the amount increases with increasing oxygen partial pressure. Wetting would therefore be expected to be improved in an oxidizing atmosphere. In fact, it has been reported that argon (oxygen level was not given) resulted in better wetting than a vacuum [77]. Moreover, a preoxidizing treatment forming silica on the surface was beneficial to wetting [78].

The width of these reaction zones can be estimated by the following relationship:

$$X = k_p t^n = k_0 t^n \exp(-Q/RT) \qquad (8)$$

where t is the brazing time, n the time exponent (usually 0.5), k_p the penetration coefficient, k_0 a constant, Q an activation energy for diffusion, R the gas constant and T the brazing temperature.

In Fig. 8, the measured reaction layer thickness for Si_3N_4–W joints with Cu–5% Ti and Cu–10% Zr brazing alloys has been plotted versus the square root of the brazing time. It is seen from the figure that growth of the reaction zone occurs more rapidly when titanium is added to the filler metal than in the case of zirconium, in spite of the lower brazing temperatures applied in the former case. Moreover, the few data obtained at prolonged brazing time reveal that the growth rate starts to level off, as shown by Fig. 9. This observation may indicate that elemental diffusion has been reduced, either by a concentration-dependent diffusivity or through impingement. Nakao *et al.* [58] suggested that impingement was caused by consumption of titanium (or zirconium) through (e.g.) the reaction with nitrogen or silicon. Under such conditions, the time exponent has been reduced to 0.5. The activation energy for diffusion, when calculated from a $\log k$–$(1/T)$ type of plot, was reported to be 318 and 429 kJ mol^{-1} for Cu–5% Ti and Cu–10% Zr alloys, respectively. According to Nakao *et al.* [58], these

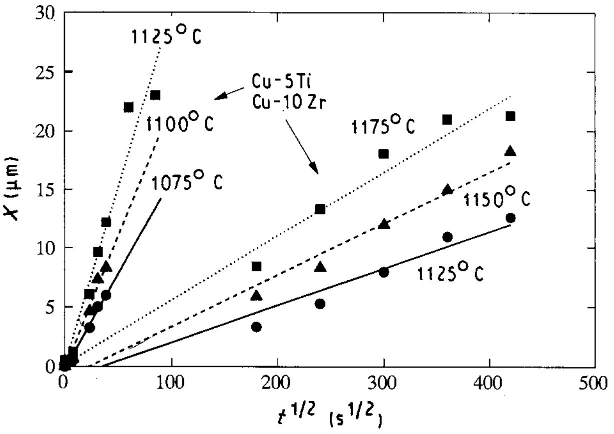

Figure 8 Effect of brazing time t on reaction zone thickness X in Si_3N_4–W joints with Cu–5% Ti and Cu–10% Zr filler metals (after Nakao *et al.* [58]).

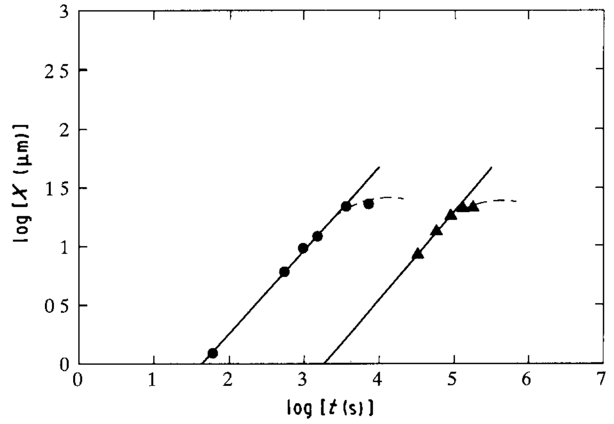

Figure 9 Effect of brazing time t on reaction zone thickness X in Si_3N_4–W joints at (●) 1125 °C (Cu–5% Ti) and (▲) 1175 °C (Cu–10% Zr) (after Nakao *et al.* [58]).

TABLE II Possible reactions between titanium- and zirconium-containing fillers and silicon-based ceramics

Reaction[a]	Free energy (kJ mol^{-1})	References
Ti(s) + $\frac{1}{2}N_2$(g) = TiN(s)	$\Delta G° = -335.8 + 0.093T$	[72, 73]
Zr(s) + $\frac{1}{2}N_2$(g) = ZrN(s)	$\Delta G° = -364 + 0.093T$	[72, 73]
Ti(s) + Si(g) = TiSi(s)	$\Delta G° = -610.9 + 0.172T$	[69]
$\frac{1}{2}$ Ti(s) + Si(g) = $\frac{1}{2}$ $TiSi_2$(s)	$\Delta G° = -538.4 + 0.150T$	[69]
Si_3N_4(s) + 9Ti(s) = 4TiN(s) + Ti_5Si_3(s)	$\Delta G° = -1370 + 0.163T$	[58]
Si_3N_4(s) + 9Zr(s) = Zr_5Si_3(s) + 4ZrN(s)[b]	$\Delta G° = -1520 + 0.201T$	[58]

[a] The symbols g and s represent gas and solid states, respectively.

[b] The zirconium nitride may have different chemical compositions, and the free energy change is dependent on the state of zirconium (the α state is represented above) [72, 73].

values are higher than the activation energy for diffusion of nitrogen in nitrides. This may, in turn, imply that the growth rate is controlled by diffusion of active metals (Ti, Zr) or Si within the reaction layer. However, determination of rate-controlling processes from calculated activation energies is not recommended, since the apparent activation energy may represent several mechanisms or rate-controlling steps (sum of activation energies). In fact, the activation energy for diffusion of titanium in copper has been reported to be 196 kJ mol^{-1} [79]. This is much lower than the value of 318 kJ mol^{-1} calculated for Cu–5% Ti alloys. Hence, it is reasonable to suggest that other mechanisms are rate-controlling. Presumably, the reaction layer may, when once formed, act as a diffusion barrier. As a consequence, several stages are probably involved in the growth process, each being characterized by an activation energy. Hence, further work is required to clarify the mechanism involved in reaction layer growth when brazing ceramics with Cu-based active metal brazes.

As mentioned previously, small amounts of Ni, Be, Cr, V, In and Co are frequently added to active brazes, and may give rise to complex elemental interactions during wetting and spreading. One of the most important aspects is that such elements may prevent extensive growth of reaction layers, as shown in Fig. 10 for brazing of AlN with Co- and Nb-containing Ag–Cu–Ti alloys. In the case of Co, however, the layer growth was primarily reduced at low brazing temperatures (< 900 °C) and short brazing times (< 10 min). In contrast, it appeared that Nb had a strong adverse effect on the layer growth, independent of temperature and time. A reduction of the thickness from 10 μm to about 2–3 μm was found when adding 10 wt% Nb to the Ag–Cu–Ti alloy. This point is illustrated in Fig. 11. Although only few data have been published, additions of Nb resulted in a joint strength improvement, which is consistent with a smaller width of the reaction zone. It was shown that Nb diffused into the Ti-rich reaction layers. Kuzumaki *et al.* [80] regarded the formation of (Ti, Nb) N as possible, since they observed a distortion of the TiN lattice when Nb was added to Ag–Cu–Ti alloys. However, since the Ti–Nb system is characterized by a full mutual solid solubility at the actual brazing temperature, an alternative hypothesis is that additions of Nb may reduce the activity of Ti. A similar effect would thus be expected for V additions. This is in sharp contrast to that obtained when adding elements with a low solubility of Ti (e.g. Sn and In) where the activity of Ti is raised (additions of Sn or In reduce the concentration of Ti required to saturate Ag–Cu or Cu brazes). In addition, the surface energy of the latter elements is low, which may facilitate segregation of Ti to the brazing alloy surface. This may, in turn, change the interface chemistry through compound formation. Although data from brazing of other ceramics with Nb-containing alloys are not yet available, they may represent a significant potential for practical applications due to the improved strength caused by the reduced reaction layer growth.

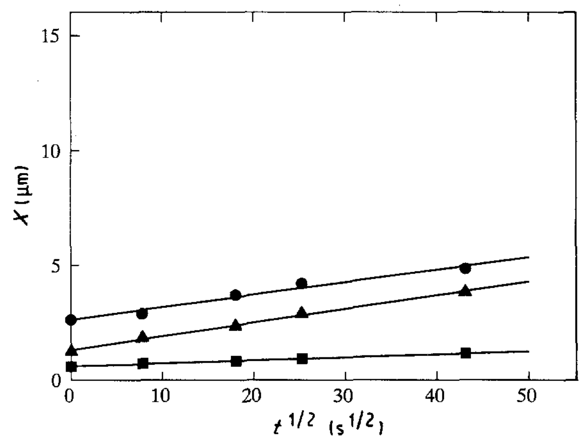

Figure 10 Effect of brazing time t on reaction zone thickness X for growth between AlN and Ag–Cu alloys at 850 °C (after Kuzumaki *et al.* [80]): (●) Ag–Cu–5Ti, (▲) Ag–Cu–5Ti–5Co, (■) Ag–Cu–5Ti–5Nb.

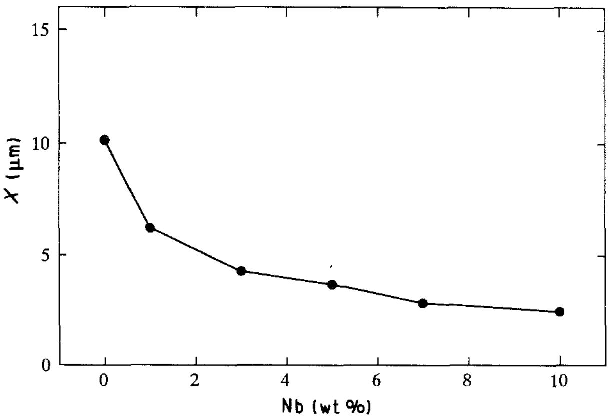

Figure 11 Effect of niobium concentration on reaction zone thickness X between AlN and Ag–Cu–5% Ti alloy brazed at 950 °C for 30 min (after Kuzumaki *et al.* [80]).

5. Properties of brazed joints

In the following section, information on the mechanical properties of directly brazed joints made with filler metals containing active elements will be given. For indirectly brazed joints (premetallized ceramic surfaces), a discussion of mechanical properties is given by Pattee [31].

5.1. Ceramic–ceramic joints

The fracture shear stress of directly brazed Si_3N_4–Si_3N_4 and SiC–SiC joints has been plotted versus the brazing temperature in Figs 12 and 13, respectively. In general, the strength tends to increase with the brazing temperature until a maximum level is reached (at 1050 and 1000–1025 °C for Si_3N_4 and SiC, respectively), which is consistent with a continuous reduction of the wetting angle with increasing temperature. However, beyond a certain temperature the joint strength is rapidly reduced. This reduction may be caused by extensive interactions between the ceramics and the Cu–Ti filler alloy, i.e. rapid growth of the reaction layer. In addition, an increase in the

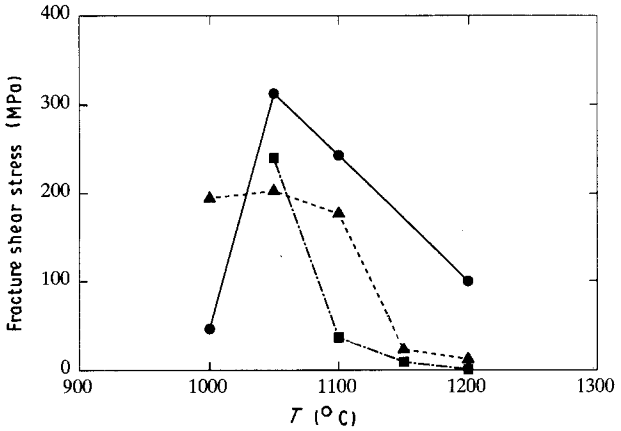

Figure 12 Effect of brazing temperature T on fracture shear stress of silicon nitride brazed with different Cu–Ti alloys for 30 min in a vacuum (after Naka *et al.* [25]): (●) 66Cu–34Ti, (▲) 50Cu–50 Ti, (■) 43Cu–57Ti.

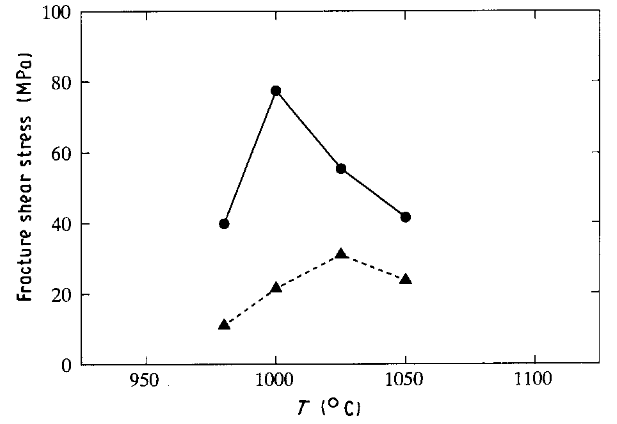

Figure 13 Effect of brazing temperature T on fracture shear stress of silicon carbide brazed with different Cu–Ti alloys for 1 min in a vacuum (after Naka *et al.* [24]): (▲) 50Cu–50Ti, (●) 43Cu–57Ti.

brazing temperature may result in an associated increase in the residual stress level.

As experienced with temperature, the strength of Si_3N_4–Si_3N_4 and SiC–SiC joints passes through a maximum with increasing brazing time. This observation is illustrated in Fig. 14. In the case of the 50 at % Cu–50 at % Ti filler alloy, the optimum brazing time is about 30 min for both silicon nitride and silicon carbide. This brazing alloy also provides reasonably high strength at elevated temperatures. An inspection of Fig. 15 reveals that the fracture shear strength is beyond 100 MPa at temperatures below 725 °C, which is sufficient for many applications. A comparison between Figs 12, 13 and 14 further reveals that silicon nitride joints possess a higher strength level than that of silicon carbide, which is in agreement with the initial base-ceramic strength level (sintered or hot-pressed). The strength reduction as a result of joining cannot be estimated since the base material properties have not been reported.

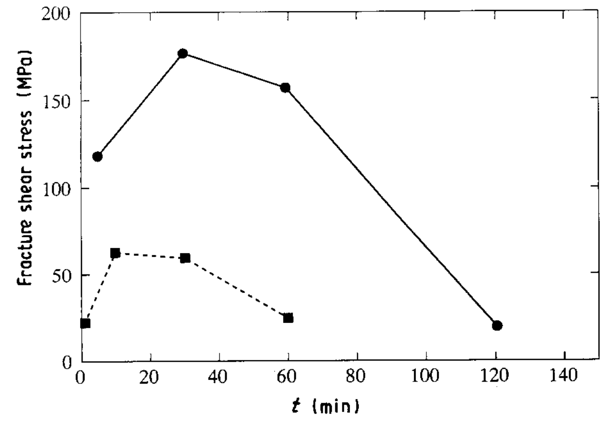

Figure 14 Effect of brazing time t on fracture shear stress of silicon carbide and silicon nitride brazed with 50 at % Cu–50 at % Ti filler alloy, vacuum brazing at (■) 1000 °C (SiC) and (●) 1100 °C (Si_3N_4) (after Naka *et al.* [24, 25]).

5.2. Ceramic–metal joints

Since ceramics in general are brittle materials, they are frequently joined to metals with a relatively high toughness and ductility. It will be seen from the following discussion that the major emphasis has been put on the development of ceramic–metal joints with a reasonably high temperature resistance. The results from mechanical testing at elevated temperatures have been plotted in Fig. 16 (alumina to copper or Kovar)

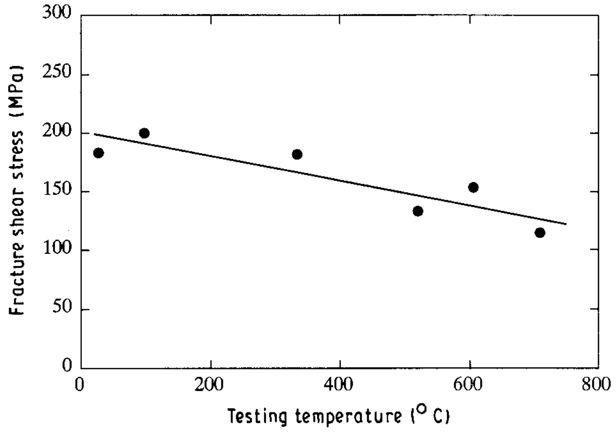

Figure 15 Effect of testing temperature on fracture shear stress of silicon nitride brazed with 50 at % Cu–50 at % Ti alloy in vacuum at 1100 °C for 30 min (after Naka *et al.* [25]).

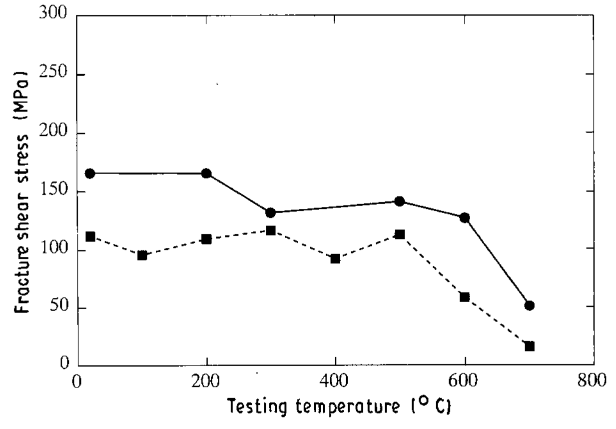

Figure 16 Effect of testing temperature on fracture shear stress of Al_2O_3–metal joints brazed with 50 at % Cu–50 at % Ti filler alloy in vacuum for 30 min; brazing temperature (■) 1025 °C for copper (after Naka *et al.* [69]) and (●) 1150 °C for Kovar (after Naka *et al.* [20]).

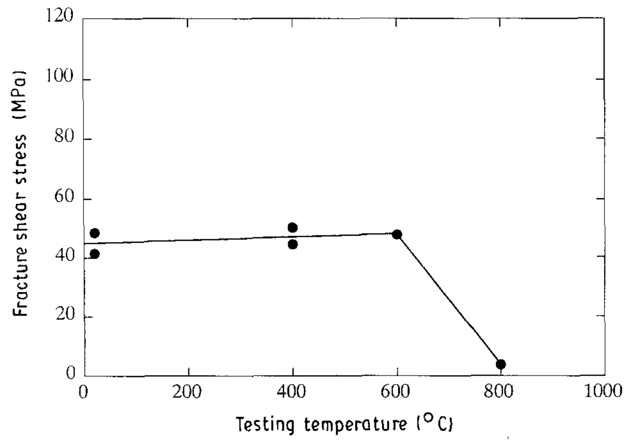

Figure 17 Effect of testing temperature on fracture shear stress of silicon carbide–stainless steel (AISI 316) joints brazed in vacuum at 950 °C for 5 min with 59 wt % Ag–23 wt % Cu–18 wt % Ti filler alloy (after Iseki *et al.* [42]).

and Fig. 17 (silicon carbide to stainless steel). In the former case, the room-temperature strength level is maintained at temperatures below 500 and 600 °C for copper and Kovar (Fe–29 wt % Ni–17 wt % Co alloy), respectively. Beyond these temperatures, the fracture shear stress has been significantly reduced. It should be noted that the maximum room-temperature bond strength of alumina–copper joints occurs for a brazing alloy titanium content of 30–40 wt % [81], which is in agreement with the level required to obtain a minimum wetting angle. A similar maximum temperature has been found for SiC–stainless steel joints (Fig. 17), although the strength level is substantially lower than that of alumina. It is therefore implied that the elevated-temperature strength of ceramic–metal joints is mainly controlled by the metal properties, since ceramics normally tolerate exposure to high temperatures before strength reduction occurs.

It should be noted that data on the strength of brazed joints are lacking for ceramic–superalloy bonds. This may be due to the fact that active brazing alloys for high-temperature applications have not yet been developed. Under such severe service conditions, the titanium-containing filler metals (Cu–Ti, Ag–Cu–Ti, Ti–Zr and Sn–Ti) do not withstand high temperatures (≈ 1000 °C) and aggressive environments. Hence, other filler metals should be considered. The nickel-based filler BNi-5 (American Welding Society Specification) has been examined in brazing silicon carbide to Inconel 600. It has been shown that extensive chemical reactions between the ceramic and the brazing filler metal may occur [82], resulting in a substantial degradation of the high-temperature properties of both SiC and Inconel 600. Although significant improvements have been made over the last decade, further developments in brazing filler metals are required to provide alloys which can meet the severe service conditions applied to ceramics.

5.3. Mismatch in thermal expansion (residual stresses)

For bonds between dissimilar materials, it is well recognized that a coefficient of thermal expansion mismatch may influence the joint strength considerably through the formation of large stresses and strains on cooling. An example of cracks formed as a result of expansion mismatch is shown in Fig. 18 for alumina brazed to a carbon–manganese steel with a 0.1 mm thick Ag–Cu–Ti alloy at 890 °C. Strength data from direct brazing of Si_3N_4 to metals or oxide ceramics (Al_2O_3, ZrO_2 and MgO) with 50 at % Cu–50 at % Ti fillers (vacuum, 1000 °C, 5 min) are presented graphically in Fig. 19 versus the difference in coefficient of thermal expansion. In spite of the large scatter observed, the joint strength tends to decrease with increasing mismatch. A similar trend has been found in the case of an aluminium brazing alloy, as shown by Fig. 20. These observations are closely linked to the formation of residual stresses at the bond interface during the brazing cycle. In the case of high brazing temperatures, the level of residual stresses may counteract the beneficial effect of temperature on wetting. This means that the joint strength may be reduced in spite of an increased wettability.

The level of residual stresses in the close vicinity of the interface between two adjacent materials 1 and 2 may be estimated roughly on the basis of the following

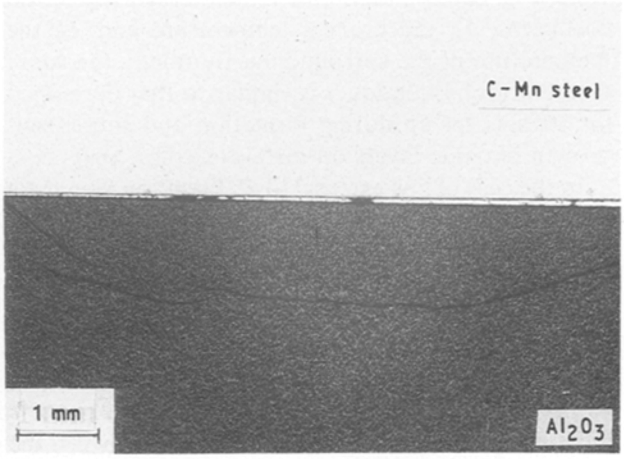

Figure 18 Example of thermally introduced cracks in an alumina–C–Mn steel joint brazed at 890 °C with a 0.1 mm thick Ag–Cu–Ti alloy.

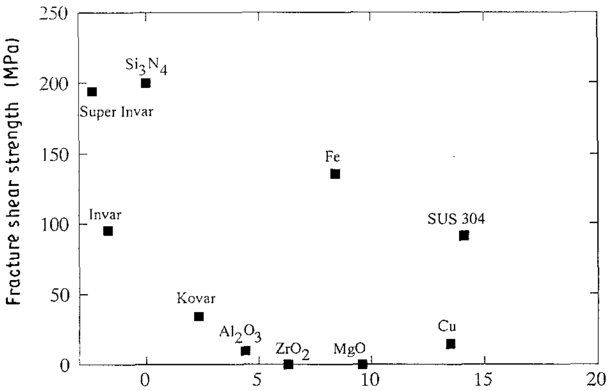

Figure 19 Effect of thermal expansion coefficient mismatch on Si_3N_4–metal and Si_3N_4–oxide ceramic joint strength; direct brazing with 50 at % Cu–50 at % Ti filler in vacuum at 1000 °C for 5 min (after Naka and Okamoto [23]).

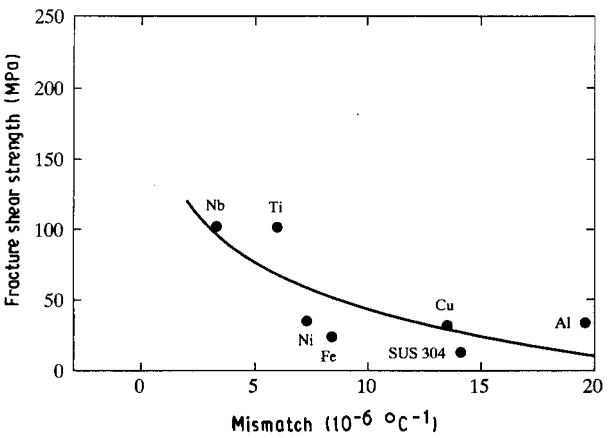

Figure 20 Effect of thermal expansion coefficient mismatch on metal–Si_3N_4 (metallized with Al) joint strength, brazed at 700 °C (after Naka *et al.* [83]).

expression [84], provided that the materials can deform elastically only (a reasonable approach for ceramics), and that the stresses generated on both sides of the reaction layer do not interfere with each other:

$$\sigma_1 = -\sigma_2 = \frac{E_1 E_2}{E_1 + E_2}(\alpha_1 - \alpha_2)(T_B - T_0) \quad (9)$$

Here E is Young's modulus, α the thermal expansion coefficient, T_B the brazing temperature and T_0 the temperature of the surroundings (normally the room temperature). Equation 9 is similar to that developed for stresses set up during formation and subsequent growth of oxide layers on metals (e.g. [85, 86]).

In the case of low external load, Equation 9 predicts that different thermal expansion may give rise to tensile stresses within the metal, and compressive stresses within the ceramic due to its lower expansion. In practice, however, the distribution of stresses in ceramic–metal joints is much more complex than that described by Equation 9 [87–89], and is non-uniform along the interface as well as within the ceramic. The most harmful effect on joint strength occurs when the tensile part of residual stresses acts on the interface or in the ceramic body. Moreover, the difference in Young's modulus may introduce stress concentrations at the interface between the dissimilar materials.

In spite of this complex situation, an illustration of the significance of residual stresses may be obtained from rough estimates using Equation 9 and the following relationship between defect size and stress level (considering the ceramic side only, and neglecting the contribution from K_{II}):

$$K_I = \frac{\pi}{2}\sigma(\pi a)^{1/2} \quad (10)$$

where K_I is the fracture toughness of ceramics, $\pi/2$ represents the defect and specimen geometry, σ is the residual stress (no external load applied), and a is the defect size (crack, pore, lack of bonding).

By inserting reasonable data for the fracture toughness of ceramics (typically $4\,MPa\,m^{1/2}$) and stress values obtained from Equation 9 and using the data contained in Table III, the critical defect size at the interface or within the ceramic body has been calculated for alumina–ceramic and alumina–metal joints. These results are shown graphically in Fig. 21. In the case of a small thermal expansion mismatch ($< 3 \times 10^{-6}\ ^{\circ}C^{-1}$), the critical defect size is estimated to be of the order of 0.05–0.25 mm. It is shown that niobium may provide the highest critical size because of a similar thermal expansion to that of alumina. This is in agreement with results obtained from diffusion bonding of alumina using niobium interlayers, where it was shown that niobium may reduce the residual stress level considerably [90].

In the case of a large mismatch, the critical crack length is reduced to a few micrometres, which is similar to previous estimates for reaction-bonded silicon nitride [91]. In practice, such defects may be present in ceramics in the form of pores. This may imply that ceramic processing (i.e. density) and surface preparation is important to provide sufficient joint mechanical properties. In fact, both Young's modulus [92] and strength [93], and hence strain at fracture, are found to be exponentially dependent on the volume fraction of pores (see the review by Moulson [94]). Therefore, it is not surprising that failure may occur in ceramic joints even without application of an

TABLE III Young's modulus, E, and coefficient of thermal expansion, α, used for calculating residual stresses (Equation 9) and critical defect size (Equation 10)

Material	Young's modulus (GPa)	Coefficient of thermal expansion ($\times 10^{-6}\ ^{\circ}C^{-1}$)
Fe	210	12.1 (10–200 °C)
Cu	110	17.2 (0–200 °C)
Invar	147	2.0 (30–100 °C)
Kovar	147	6.0 (30–500 °C)
SUS 304	210	17.8 (0–300 °C)
Al_2O_3	360	8.1 (25–)
ZrO_2	131	10.0 (25–)
MgO	85	13.3 (25–)
Si_3N_4	294	3.7 (40–800 °C)
Inconel 600	217	6.7 (25–)
Ti	117	9.7 (25–600 °C)
W	350	4.6 (25–500 °C)
Mo	329	5.7 (25–500 °C)
Cr	210	11.3 (25–600 °C)
Ni	168	11.0 (25–600 °C)
Nb	112	7.0 (25–)

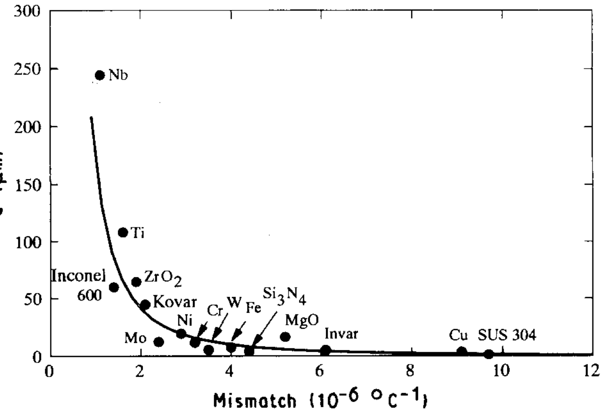

Figure 21 Effect of thermal expansion coefficient mismatch on critical defect size *a* (calculated from Equation 10) in direct brazing of Al_2O_3–metal and Al_2O_3–ceramic joints at 900 °C.

external load. Moreover, it is implied that testing of ceramics requires an adequate test technique, which besides adherence also includes an assessment of the flaw size (e.g. pores, internal cracks, lack of bonding). A discussion of these aspects is given by Moorhead and Becher [95]. In addition, design data with sufficient reliability and quality are still lacking [96].

6. Summary

The scientific principles involved in the brazing of ceramics have been discussed. In general, wetting seems to be the limiting factor to obtain sufficient adherence. This fact has led to the development of various techniques to metallize the ceramic surfaces prior to brazing (indirect brazing). Recent advances have, however, resulted in new types of brazing alloy, which provide sufficiently low contact angles due to the addition of active elements. These are essentially Ag–Cu, Ag or Cu brazes with additions of Ti, and Sn-based solders. In this case premetallization is not necessary, which means that direct brazing is possible. The joining operation is normally performed in vacuum environments or a high-purity inert gas atmosphere to prevent the active metal constituent from reacting with oxygen, hydrogen, nitrogen or carbon.

The mechanical properties of directly brazed ceramic–ceramic and ceramic–metal joints have been discussed as functions of key parameters such as temperature and time. In the brazing of dissimilar materials, the mismatch in coefficient of thermal expansion between the joint members may result in the formation of large residual stresses. This may, in turn, reduce the mechanical integrity of the joint. Under such conditions, the maximum allowable flaw size to avoid initiation of unstable fracture become very small, indicating that failure may occur even in the absence of external load. Hence, the test techniques employed to characterize ceramic–metal bonds should include an assessment of the critical flaw size, in addition to adherence.

Acknowledgement

The author wishes to thank the Royal Norwegian Council for Scientific and Industrial Research (NTNF) for financial support (Contract No. MT3001.25312).

References

1. W. D. HARKINS, "The Physical Chemistry of Surface Films" (Reinhold, New York, 1952) p. 175.
2. W. D. KINGERY, *Amer. Ceram. Soc. Bull.* **35** (1956) 108.
3. N. YOSHIMI, H. NAKAE and H. FUJII, *Mater. Trans. JIM* **31** (1990) 141.
4. J. F. LANCASTER, "Metallurgy in Welding", 3rd Edn (Allen & Unwin, London, 1980) p. 89.
5. A. KASAMA, T. IIDA and Z. MORITA, *J. Jap. Inst. Met.* **40** (1976) 1030.
6. S. M. KAUFMANN and T. J. WHALEN, *Acta Metall.* **13** (1965) 797.
7. D. W. G. WHITE, *Metall. Trans.* **2** (1971) 367.
8. I. LAUERMANN, G. METZGER and F. SAUERWALD, *Z. Phys. Chem.* **216** (1961) 43.
9. G. BERNARD and C. H. P. LUPIS, *Metall. Trans.* **2** (1971) 555.
10. W. KRAUS, F. SAUERWALD and M. MICHALCE, *Z. Anorg. Chem.* **18** (1929) 353.
11. Z. METZGER, *Z. Phys. Chem.* **211** (1959) 1.
12. W. GANS, F. PAWLEK and A. ROPENACK, *Z. Metallk.* **54** (1963) 147.
13. B. C. ALLEN and W. D. KINGERY, *Trans. Met. Soc. AIME* **215** (1959) 30.
14. S. K. RHEE, *J. Amer. Ceram. Soc.* **53** (1970) 639.
15. K. NOGI, K. OISHI and K. OGINO, *Mater. Trans. JIM* **30** (1989) 137.
16. T. E. O'BRIEN and A. D. CHAKLADER, *J. Amer. Ceram. Soc.* **57** (1974) 329.
17. F. P. BOWDEN and E. K. RIDEAL, *Proc. R. Soc.* **120** (1928) 241.
18. R. N. WENXEL, *Ind. Eng. Chem.* **28** (1936) 988.
19. M. NAKA, K. ASAMI, I. OKAMOTO and Y. ARATA, *Trans. JWRI* **12** (1983) 145.
20. M. NAKA, T. TANAKA, I. OKAMOTO and Y. ARATA, *ibid.* **12** (1983) 177.
21. M. NAKA, K. SAMPATH, I. OKAMOTO and Y. ARATA, *ibid.* **12** (1983) 181.
22. *Idem*, in Proceedings of International Conference, "Joining of Metals", Denmark, 1984, edited by O. Al-Erhayen, p. 169.
23. M. NAKA and I. OKAMOTO, *Trans. JWRI* **14** (1985) 29.
24. M. NAKA, T. TANAKA and I. OKAMOTO, *J. High Temp. Soc.* **11** (1985) 218.
25. *Idem*, *Trans. JWRI* **15** (1986) 49.
26. *Idem*, *ibid.* **16** (1987) 83.
27. H. MIZUHARA and K. MALLY, *Weld. J.* **64** (1985) 27.
28. B. WIELAGE, in Proceedings of 2nd International Symposium, "Ceramic Materials and Components for Engines", Lübeck-Travemunde, Germany, April 1986, p. 391.
29. A. J. MOORHEAD and H. KEATING, *Weld. J.* **65** (1986) 17.
30. E. LUGSCHEIDER and W. TILLMANN, *ibid.* **69** (1990) 416-s.
31. H. PATTEE, *Weld. Res. Counc. Bull.* **178** (1972).
32. *Idem*, in "Source Book on Brazing and Brazing Technology" (American Society for metals, 1980) p. 315.
33. C. W. FOX and G. M. SLAUGHTER, *Weld. J.* **43** (1964) 591.
34. J. E. SIEBELS, in "Progress in Nitrogen Ceramics", edited by F. L. Riley (Nijhoff, The Netherlands, 1983) p. 455.
35. A. J. MOORHEAD, C. S. MORGAN, J. J. WOODHOUSE and R. W. REED, *Weld. J.* **60** (1981) 17.
36. H. MIZUHARA and E. HUEBEL, *ibid.* **65** (1986) 43.
37. B. WIELAGE, R. DAMMER and P. DYRDA, *Pract. Met.* **26** (1989) 133.
38. T. KUZUMAKI, T. ARIGA, Y. MIYAMOTO and T. KOBAYASHI, *ISIJ Int.* **30** (1990) 403.
39. D. A. CANONICO, N. C. COLE and G. M. SLAUGHTER, *Weld. J.* **56** (1977) 31.
40. M. NAKA, I. OKAMOTO, T. NISHINO and S. URAI, *Trans. JWRI* **18** (1989) 27.
41. R. STANDING and M. NICHOLAS, *J. Mater. Sci.* **13** (1978) 1509.
42. T. ISEKI, H. MATSUZAKI and J. K. BOADI, *Amer. Ceram. Soc. Bull.* **64** (1985) 322.
43. J. P. HAMMOND, S. A. DAVID and M. L. SANTELLA, *Weld. J.* **67** (1988) 227-s.
44. E. LUGSCHEIDER, H. KRAPPITZ and H. MIZUHARA, *Fortschr. Ber. Deut. Keram. Ges.* **1** (1985) 199.
45. E. LUGSCHEIDER, H. KRAPPITZ and R. PETERS, *Pract. Met.* **24** (1987) 195.
46. D. T. LIVEY and P. MURRAY, in Proceedings of 2nd Plansee Seminar, Reutte, Austria, 1955, p. 375.
47. R. D. CARNAHAN, T. L. JOHNSTON and C. H. LI, *J. Amer. Ceram. Soc.* **41** (1958) 343.
48. S. M. WOLF, A. P. LEVITT and J. I. BROWN, *Chem. Eng. Progr.* **62** (1966) 74.
49. J. J. BRENNAN and J. A. PASK, *J. Amer. Ceram. Soc.* **51** (1968) 569.
50. J. A. CHAMPION, B. J. KEENE and J. M. SILLWOOD, *J. Mater. Sci.* **4** (1969) 39.

51. H. JOHN and H. HAUSNER, *Int. J. High Technol. Ceram.* **2** (1986) 73.
52. M. NAKA, Y. HIRONO and I. OKAMOTO, *Trans. JWRI* **29** (1984) 29.
53. M. UEKI, M. NAKA and I. OKAMOTO, *J. Mater. Sci.* **23** (1988) 2983.
54. R. R. KAPOOR and T. W. EAGAR, *Metall. Trans.* **20B** (1989) 919.
55. *Idem, J. Amer. Ceram. Soc.* **72** (1989) 448.
56. "Metals Handbook", 8th Edn, Vol. 8 (1973) p. 300.
57. A. R. MIEDEMA, F. R. de BOER and R. BOOM, *CALPHAD* **1** (1977) 341.
58. Y. NAKAO, K. NISHIMOTO and K. SAIDA, *Trans. JWS* **20** (1989) 66.
59. H. PULFRICH, US Patent 2 163 407 (1939).
60. H. PULFRICH and R. MAGNER, US Patent 2 163 410 (1939).
61. H. J. NOLTE, and R. F. SPURCK, *Telev. Eng.* **1** (1950) pp. 14–16, 18, 39.
62. R. M. FULLRATH and E. L. HOLLAR, *Amer. Ceram. Soc. Bull.* **47** (1968) 493.
63. L. REED and R. A. HUGGINS, *J. Amer. Ceram. Soc.* **48** (1965) 421.
64. L. REED, "Electronic Ceramics", Special Publication No. 3 (American Ceramic Society, Columbus, Ohio, 1969).
65. M. E. TWENTYMAN, *J. Mater. Sci.* **10** (1975) 765.
66. M. E. TWENTYMAN and P. POPPER, *ibid.* **10** (1975) 777.
67. W. H. KOHL, "Handbook of Materials and Techniques for Vacuum Devices" (Reinhold, New York, 1967) p. 451.
68. D. R. MILNER, *Br. Weld. J.* **5** (1958) 90.
69. M. NAKA, K. ASAMI and I. OKAMOTO, *Trans. JWRI* **15** (1986) 253.
70. J. L. MURRAY and H. A. WRIEDT, *Bull. Alloy Phase Diag.* **8** (1987) 148.
71. A. CEZAIRLIYAN, *High Temp. High Press.* **1** (1969) 517.
72. O. KUBASCHEWSKI and C. B. ALCOCK, "Metallurgical Thermochemistry", 5th Edn, International Series on Materials Science Technology, Vol. 24 (Pergamon, 1979).
73. W. BILTZ and R. JUZA, *Z. anorg. Chem.* **190** (1930) 161.
74. J. K. BOADI, T. YANO and T. ISEKI, *J. Mater. Sci.* **22** (1987) 2431.
75. M. NAKA, H. MORI, M. KUBO, I. OKAMOTO and H. FUJITA, *J. Mater. Sci. Lett.* **5** (1986) 696.
76. X. S. NING, K. SUGANUMA, M. MORITA and T. OKAMOTO, *Phil. Mag. Lett.* **55** (1987) 93.
77. K. SUGANUMA, T. OKAMOTO, M. KOIZUMI and M. SHIMADA, *J. Mater. Sci.* **22** (1987) 1359.
78. M. MORITA, K. SUGANUMA and T. OKAMOTO, *J. Mater. Sci. Lett.* **6** (1987) 474.
79. Y. IIJIMA, K. HOSHINO and K. HARANO, *Metall. Trans.* **8A** (1977) 997.
80. T. KUZUMAKI, T. ARIGA and Y. MIYAMOTO, *ISIJ Int.* **30** (1990) 1135.
81. T. KUZUMAKI, T. ARIGA, Y. MIYAMOTO and T. KOBAYASHI, *ibid.* **30** (1990) 403.
82. J. R. McDERMID, M. D. PUGH and R. A. L. DREW, *Metall. Trans.* **20A** (1989) 1803.
83. M. NAKA, M. KUBO and I. OKAMOTO, *Trans. JWRI* **18** (1989) 33.
84. X. S. NING, T. OKAMOTO, Y. MIYAMOTO, A. KOREEDA and K. SUGANUMA, *J. Mater. Sci.* **24** (1989) 2865.
85. D. L. DOUGLASS, *J. Less-Common Met.* **5** (1963) 151.
86. *Idem*, "Oxidation of Metals and Alloys" (ASM, Metals Park, Ohio, 1970) p. 152.
87. M. TOYODA, T. KOMATSU, K. SATOH and M. NAYAMA, International Institute of Welding Doc. X-1161-88 (1988).
88. H. MURUKAWA and Y. UEDA, *Trans. JWRI* **18** (1989) 133.
89. K. SUGANUMA, T. OKAMOTO, M. KOIZUMI and M. SHIMADA, *Commun. Amer. Ceram. Soc.* **12** (1985) 334.
90. *Idem, Adv. Ceram. Mater.* **1** (1986) 356.
91. A. G. EVANS and R. W. DAVIDGE, *J. Mater. Sci.* **5** (1970) 314.
92. E. RYSHKEWITCH, *J. Amer. Ceram. Soc.* **36** (1953) 65 (with discussion by W. Duckworth).
93. D. S. THOMPSON and P. L. PRATT, *Proc. Br. Ceram. Soc.* **6** (1966) 37.
94. A. J. MOULSON, *J. Mater. Sci.* **14** (1979) 1017.
95. A. J. MOORHEAD and P. F. BECHER, *Weld. J.* **66** (1987) 26-s.
96. C. F. LEWIS, *Mater. Engng* (1988) 41.

Received 1 March
and accepted 21 August 1991